Chinese Journal of Oceanology and Limnology
Vol. 33 No. 5, P. 1124-1131, 2015
http://dx.doi.org/10.1007/s00343-015-4126-6

Effect of wave spectrum width on the probability density distribution of wind-wave heights*

LIU Yahao (刘亚豪)[1, 2], HOU Yijun (侯一筠)[1, 2, **], HU Po (胡珀)[1, 2], LIU Ze (刘泽)[1, 2]

[1] *Key Laboratory of Ocean Circulation and Waves* (*KLOCAW*), *Chinese Academy of Sciences*, *Qingdao 266071*, *China*
[2] *Institute of Oceanology*, *Chinese Academy of Sciences*, *Qingdao 266071*, *China*

Received May 31, 2014; accepted in principle Jul. 22, 2014; accepted for publication Sep. 1, 2014

Abstract The probability distribution of wave heights under the assumption of narrowband linear wave theory follows the Rayleigh distribution and the statistical relationships between some characteristic wave heights, derived from this distribution, are widely used for the treatment of realistic wind waves. However, the bandwidth of wave frequency influences the probability distribution of wave heights. In this paper, a wave-spectrum-width parameter B was introduced into the JONSWAP spectrum. This facilitated the construction of a wind-wave spectrum and the reconstruction of wind-wave time series for various growth stages, based on which the probability density distributions of the wind-wave heights were studied statistically. The distribution curves deviated slightly from the theoretical Rayleigh distribution with increasing B. The probability that a wave height exceeded a certain value was clearly smaller than the theoretical value for $B\geq0.3$, and the difference between them increased with the threshold value. The relation between the H_s/σ ratio and B was investigated statistically, which revealed that the H_s/σ ratio deviated from 4.005 and declined with B. When B reached 0.698 1, the H_s/σ ratio was 3.825, which is about 95.5% of its original value. This indicates an overestimation in the prediction of H_s from $H_s=4.005\sigma$, and provides a potential method for improving the accuracy of the H_s remote sensing retrieval algorithm, critical for extremely large waves under severe sea states.

Keyword: wave-spectrum width; probability distribution of wave heights; significant wave height

1 INTRODUCTION

The probability distribution of wave heights is of great practical importance for coastal and offshore engineering. Longuet-Higgins (1952) first presented the idea that theoretically wave heights should follow the Rayleigh distribution. This idea was based on the two following assumptions: 1) that the wave comprises the sum of sinusoids in random phase and 2) that the frequencies of these sine waves are concentrated in a narrow band. Under the Rayleigh distribution, the probability P that the wave height H exceeds a given value H_0 is given by

$$P\left(H > H_0\right) = \exp\left(-\frac{H_0^2}{H_{\text{rms}}^2}\right), \quad (1)$$

where H_{rms} denotes the root mean-square wave height, given as $H_{\text{rms}}=(8m_0)^{1/2}$ following Cartwright and Longuet-Higgins (1956), m_0 denotes the lowest moment of the frequency spectrum.

Although the Rayleigh distribution has shown surprisingly good agreement with many field observations, even if the assumptions were not fulfilled exactly, more and more researchers have reported that it does not fit their data so well (Earle, 1975; Haring et al., 1976; Chakrabarti and Cooley, 1977; Forristall, 1978) and therefore, some other expressions of the distribution have been proposed. Forristall (1978) proposed an empirical Weibull distribution to fit his storm wave data gathered in the Gulf of Mexico. Longuet-Higgins (1980) revised the theoretical relation between H_{rms} and m_0 by adding a small free-

* Supported by the National High Technology Research and Development Program of China (863 Program) (No. 2013AA09A505), the National Natural Science Foundation of China (Nos. U1133001, 41376027, 41406017), and the NSFC-Shandong Joint Fund for Marine Science Research Centers (No. U1406401)
** Corresponding author: yjhou@qdio.ac.cn

wave perturbation into the narrow-band spectrum to fit with the observations from the same data set. He attributed the deviation of $H_{rms}/(8m_0)^{1/2}$ from unity to the presence of free background "noise" waves outside the dominant spectral peak, and Larsen (1981) confirmed this result with observations obtained off the Washington continental shelf. Naess (1985) further derived a one-parameter Rayleigh distribution function of wave heights, employing a parameter linked with the dominant wave period to show the effect of bandwidth on the distribution function.

In reality, sea surface wind waves do not always fulfill Longuet-Higgins' two assumptions. Much research has been performed on the statistical distribution of nonlinear random waves with regard to the shapes of wave components (Longuet-Higgins, 1963; Tayfun, 1980; Huang et al., 1983; Hou et al., 2006; Alkhalidi and Tayfun, 2013; Izadparast and Niedzwecki, 2013). However, the effect of a realistic wind-wave spectral bandwidth on the probability distribution of wave heights has been rarely studied. Goda and Kudaka (2007) defined a spectral shape parameter κ, associated with the spectral characteristics of a wave series, to study the influence of bandwidth on the distribution of wave heights. Boccotti (2012) improved Naess' expression by defining a dimensionless variable β that is related to wave height and that has the same asymptotic distribution in Gaussian sea states with a very large variety of bandwidths and spectrum shapes. The results from his formula are identical to a huge mass of wave observations; however, because the parameters in formulas have to be calculated from wave-measurement records, not all these expressions can be easily used in wind-wave predictions.

In this paper, the JONSWAP spectrum (Hasselmann et al., 1973), which can depict the spectral features of the entire growth stages of wind waves, is taken as a typical spectrum of real wind waves. The spectrum width B, defined by Hou and Wen (1990), is introduced to describe the growth state and thus, the spectrum bandwidth of the wind waves. The advantage of using B is that it can be integrated into the expression of the wind-wave spectrum as a spectral factor and thus, be derived conveniently from an empirical relation with wind fetch, instead of field observations, during wind-wave predictions (Wang and Hou, 2008). In this study, a set of numerical experiments was conducted to inspect the effect of B on the probability distribution of wind-wave heights by statistically analyzing the simulated wave series generated from the wind-wave spectrum containing B.

One of the most important applications of wave height probability distribution is to determine the significant wave height H_s from the lowest moment of spectrum m_0. Under the Rayleigh distribution, H_s is given by

$$H_s = 4.005\sqrt{m_0} \approx 4\sqrt{m_0} = 4\sigma\,, \tag{2}$$

where σ denotes the root mean square surface elevation, which can be derived from the waveform of the backscatter signals received by the satellite radiometer, under the assumption that the spatial possibility density of sea surface elevation obeys a Gaussian distribution. Currently, this relation is still used in operational altimeter remote sensing retrieval algorithms, for sea surface wave heights, to estimate the values of H_s from $m_0^{1/2}$. However, according to previous theoretical studies (Tayfun, 1990; Tayfun and Fedele, 2007; Alkhalidi, 2012), the existence of both nonlinearity and bandwidth effects lowers the $H_s/m_0^{1/2}$ ratio from 4.005, and introduces systematic error into the H_s product based on Eq.2. Although some revised formulas do provide values for the $H_s/m_0^{1/2}$ ratio that are more accurate (Goda and Kudaka, 2007), they are unsuitable for remote sensing applications because of the difficulty in evaluating their parameters. In the following sections, we will see that for the conditions of realistic wind waves, the error from Eq.2 increases with the growth of wind waves and the increase of B, which indicates a loss of accuracy in the evaluation of H_s, especially for severe sea states when the magnitudes of the waves are larger than usual.

2 FORMULATION AND METHOD

2.1 Construction of wind-wave spectrum

The basic form of a wind-wave spectrum employed here is the JONSWAP spectrum. The spectral model takes the form (Hasselmann et al., 1973)

$$S(\omega) = \frac{\alpha g^2}{\omega^5}\exp\left[-\frac{5}{4}\left(\frac{\omega}{\omega_0}\right)^{-4}\right]\gamma^{\delta}\,, \tag{3}$$

in which

$$\delta = \exp\left[-\frac{(\omega/\omega_0 - 1)^2}{2\sigma^2}\right], \tag{4}$$

where α is a non-dimensional parameter determined by wind speed and fetch, g denotes gravitational acceleration, ω denotes wave frequency and ω_0 is the frequency at the spectral peak, σ=0.07 for $\omega \le \omega_0$ and σ=0.09 for $\omega > \omega_0$, and the term γ^{δ} is the peak

enhancement factor. The value of factor γ varies from unity to infinity and it is 3.3 for the mean JONSWAP spectrum. When $\gamma \rightarrow$ infinity, the spectral form should asymptotically approach the Dirac delta function, which represents a monochromatic wave. When $\gamma \rightarrow 1$, the spectral form becomes the Pierson-Moskowitz spectrum for large fetch, which represents fully grown wind waves (Pierson Jr. and Moskowitz, 1964). Thus, by varying the value of γ, the JONSWAP spectrum can represent wind waves in various growth stages.

For $\omega=\omega_0$, we have

$$S(\omega_0)=\frac{\alpha g^2}{\omega_0^5}\exp\left(-\frac{5}{4}\right)\gamma\,. \tag{5}$$

Equation 3 can then be rewritten as

$$S(\omega)=S(\omega_0)\left(\frac{\omega}{\omega_0}\right)^{-5}\exp\left[-\frac{5}{4}\left(\frac{\omega}{\omega_0}\right)^{-4}-1\right]\gamma^{\delta-1}. \tag{6}$$

The wave-spectrum width B is defined by Hou and Wen (1990) as

$$B=\frac{m_0}{\omega_0 S(\omega_0)}. \tag{7}$$

The value of B is equal to the ratio of geometric area between the area under the spectrum curve and the square with sides ω_0 and $S(\omega_0)$. Based on Eq.7, the spectrum form becomes

$$S(\omega)=\frac{m_0}{\omega_0 B}\left(\frac{\omega}{\omega_0}\right)^{-5}\exp\left[-\frac{5}{4}\left(\frac{\omega}{\omega_0}\right)^{-4}-1\right]\gamma^{\delta-1}. \tag{8}$$

The spectrum form is determined by three parameters: B, m_0, and ω_0. If $\tilde{S}(\tilde{\omega})=S(\omega)\omega_0/m_0$ and $\tilde{\omega}=\omega\ \ \omega$ are assigned, the non-dimensionalized form of Eq.8 becomes

$$\tilde{S}(\tilde{\omega})=\frac{1}{\mathrm{B}}\tilde{\omega}^{-5}\exp\left[-\frac{5}{4}\left(\tilde{\omega}^{-4}-1\right)\right]\gamma^{\exp\left[-\frac{(\tilde{\omega}-1)^2}{2\sigma^2}\right]-1}, \tag{9}$$

in which the symbols with wavy overlines (~) denote the non-dimensional terms.

The value of B can be calculated using

$$B=\int_0^\infty \tilde{\omega}^{-5}\exp\left[-\frac{5}{4}\left(\tilde{\omega}^{-4}-1\right)\right]\gamma^{\exp\left[-\frac{(\tilde{\omega}-1)^2}{2\sigma^2}\right]-1}\mathrm{d}\tilde{\omega}. \tag{10}$$

The dependence relationship between B and γ is shown in Fig.1. For the JONSWAP spectrum, $B\rightarrow 0$ when $\gamma\rightarrow$infinity, while $B\rightarrow 0.6981$ when $\gamma\rightarrow 1$. As γ performs as a monotonous decreasing function of B, the shape of the spectrum described by Eq.9 actually has only one parameter, i.e., B. For the dimensional spectrum described by Eq.8, the parameters m_0 and ω_0 only decide the magnitude and peak location, but they are not related to the shape of the spectrum form. Hence, one can say that the shape of the JONSWAP spectrum is completely determined by B.

Our objective is to investigate the effect of B, i.e., the shape of the spectrum curve, on the probability distribution of wind-wave heights. Therefore, we set $m_0=1$ and $\omega_0=1$ and take the spectrum form as described by Eq.9 for simplification. The spectrum for $B=0.10$ ($\gamma=149.13$), 0.698 1 ($\gamma=1$), and 11 other values between these two extreme ones are presented in Table 1.

2.2 Reconstruction of wave surface

After the construction of the wind-wave spectrum, the next step is to transform the spectrum "back" to the time series of surface displacement at a fixed spot. Here, we assume the surface displacement is a stationary stochastic process with an expected zero value, which still comprises the sum of an infinite number of sinusoids in random phase, but this time, the frequencies of these waves are not necessarily concentrated within a narrow band. Then, using the Fourier-Stieljes integral, this surface displacement $\zeta(t)$ can be given by

$$\zeta(t)=\int_0^\infty \cos(\omega t+\varepsilon)\sqrt{4S(\omega)\mathrm{d}\omega}\,, \tag{11}$$

where phase ε follows a uniform distribution on the interval $[-\pi, \pi)$. This formula is the same in form as Eq.8 of Goda (1970). The formula in discrete form employed in our simulations is

$$\zeta(t)=\sum\nolimits_\omega \cos(\omega t+\varepsilon)\sqrt{4S(\omega)\Delta\omega}\,. \tag{12}$$

The summation was processed with $\Delta\omega=0.01$ for ω in the interval [0, 13], which contains more than 99.99% of the total energy. The time interval Δt was set to 0.05 s and the length of the time series was 1 000 s. The wave heights were extracted from the time series, following which H_s and H_{rms} were calculated statistically from the wave height sets. For each spectrum form, 300 000 time series with different ε were generated and the average values of the statistical terms given as final results (Table 1).

3 RESULT

3.1 Effect of B on probability distribution of wave heights

The probability density distribution functions of wind-wave heights with different values of B were evaluated, some of which are shown in Fig.2. The wave height H is normalized by dividing by σ for the

Table 1 Values of statistical parameters for various *B*

B	γ	H_{rms}/m	$H_s/m_0^{1/2}$	ε	ν	$\kappa(T_{01})$	$r(T/2)$
0*	∞	8	4.005	0	0	1	-1
0.10	1.49×10^{2}	7.933	3.962	0.521	0.148	0.994	-0.969
0.15	2.07×10^{1}	7.783	3.924	0.749	0.366	0.975	-0.877
0.20	8.96	7.660	3.897	0.794	0.532	0.962	-0.798
0.25	5.40	7.577	3.880	0.809	0.656	0.954	-0.746
0.30	3.77	7.520	3.867	0.815	0.750	0.949	-0.711
0.35	2.86	7.479	3.857	0.818	0.825	0.945	-0.687
0.40	2.29	7.449	3.849	0.819	0.886	0.943	-0.669
0.45	1.89	7.428	3.843	0.820	0.937	0.941	-0.657
0.50	1.61	7.410	3.838	0.821	0.980	0.939	-0.647
0.55	1.40	7.395	3.834	0.821	1.017	0.938	-0.639
0.60	1.24	7.384	3.831	0.821	1.049	0.937	-0.633
0.65	1.10	7.375	3.828	0.821	1.078	0.936	-0.628
0.6981	1.00	7.368	3.825	0.820	1.102	0.935	-0.624

* Data in this line are not calculated from simulated waves, but theoretical values for narrowband waves. Definition of the last four parameters is in Section 4.

convenience of comparison. The probability curves for wind waves generally exhibit good similarity with the Rayleigh distribution, which is the theoretic distribution of Longuet-Higgins' narrowband linear waves. For newly created wind waves (e.g., B=0.1), the distribution of wave heights is slightly more concentrated in the peak area and the peak value is slightly higher than the Rayleigh peak value. However, with the growth of wind waves, the peak value falls back while the location of the curve peak shifts rightwards. At the same time, the probability of the occurrence of small wave heights rises whereas that for large wave heights declines.

Figure 3 shows the deviation of wind-wave height distributions from the Rayleigh distribution. It can be seen that on each line there are three zero-crossing points, in addition to those for zero and extremely large wave heights. For all values of B, the deviation curves are initially positive when the wave heights are small. They then pass below zero and undergo another vibration, before finally gradually approaching zero again. The deviation curve for small B (i.e., B=0.1) is distinct from the others with regard to phase; its first peak-valley "period" takes only half the wave-height domain of the others and its third zero-crossing point approximately encounters the second of the others, around the point H/σ=1. The B=0.1 curve approaches its maximum value near H/σ=2, at which point the others have just passed their lowest values; the maximum values of which are located around H/σ=3.

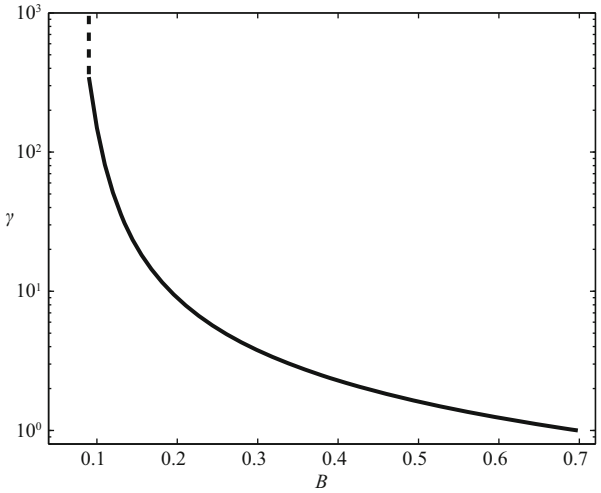

Fig.1 Dependence relationship between *B* and *γ*

When H/σ>5, the curve forms for all values of B are almost the same. The similarities of the deviation curves for B>0.3 indicate that the probability distributions of wind-wave heights vary quickly when the waves are just generated, but then achieve quasi-stationary states and do not vary much during the entire growth stage.

The exceedance probabilities $P(H>H_0)$ with different values of B are shown in Fig.4. As the peak frequencies of the spectra are set to unity and the lengths of the time series are 1 000 s, there are on average about 1 000/2π≈160 wave heights recorded in one series. Exceedance probabilities smaller than

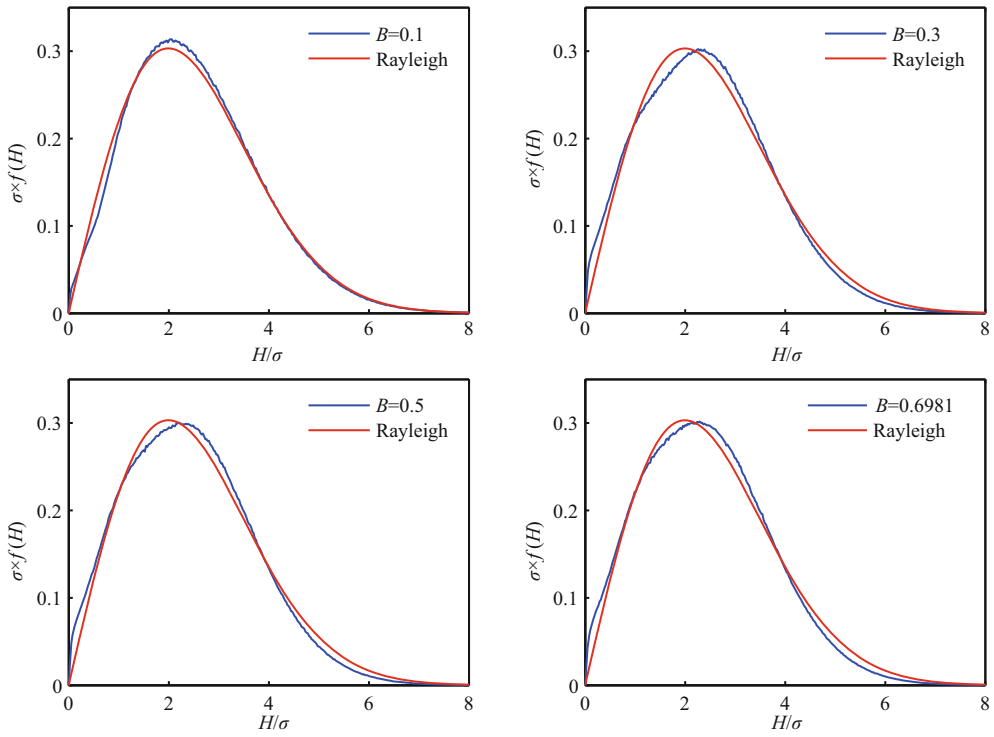

Fig.2 Probability density distributions of wind-wave heights for various *B*

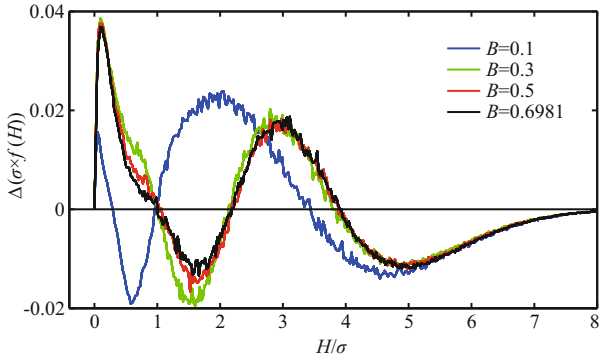

Fig.3 Differences between simulated and theoretical (Rayleigh) distributions

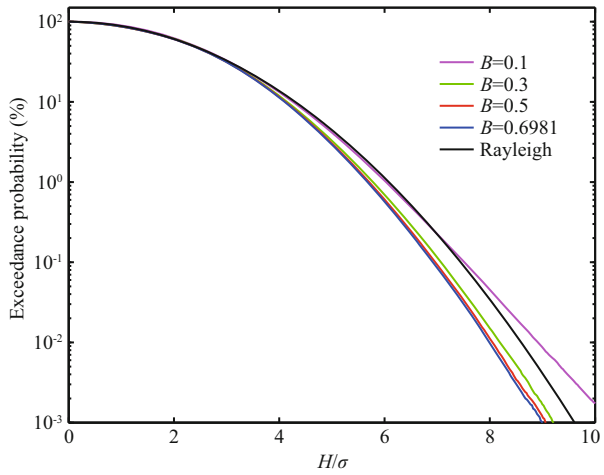

Fig.4 Probabilities of exceedance for various *B*

1/160=0.625% cannot be counted from a single time series, but they are calculated statistically; therefore, these data, whose accuracies are questionable, are shown only for reference.

The distributions of exceedance probability for different values of B show similar features to the probability density distributions. For newly created wind waves (e.g., B=0.1), the exceedance probability curve is quite close to the theoretical narrowband curve; however, for larger values of B, the curves exhibit obvious deviations. The probabilities of exceeding a certain height for real wind waves are lower than for the Rayleigh distribution, indicating that the prediction of characteristic wave heights for wind waves by the Longuet-Higgins theoretical relation will induce some overestimation; the smaller the exceedance probability, the larger the overestimation. The value of $H_{1\%}$ for B=0.698 1 is 6.4% smaller than that for the Rayleigh distribution.

3.2 Effect of B on $H_{rms}/m_0^{1/2}$ and $H_s/m_0^{1/2}$ ratios

There are some important relations between the characteristic wave heights derived from the probability distributions, to which considerable attention is paid. One of these is the ratio between H_{rms} and $m_0^{1/2}$, which has long been seen as an indicator of the influence of frequency bandwidth (Longuet-Higgins, 1980). For narrowband waves, the expected

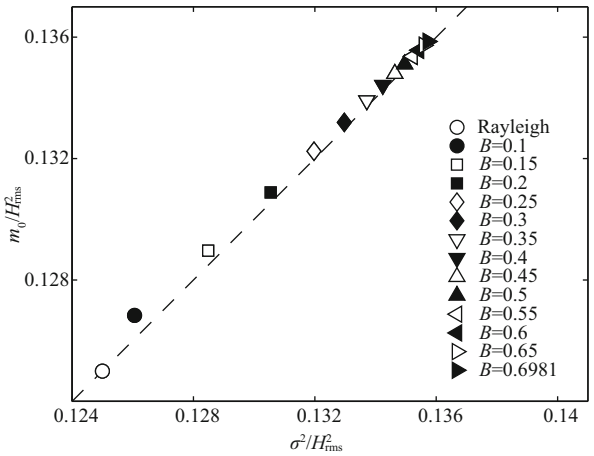

Fig.5 Comparison between m_0 and σ^2

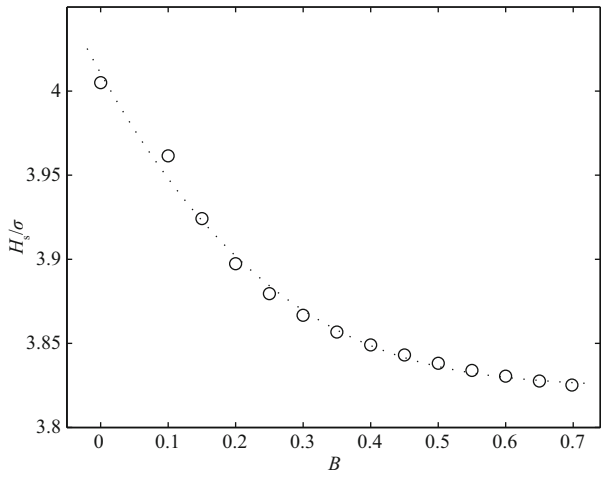

Fig.6 Dependence of H_s/σ ratio on B

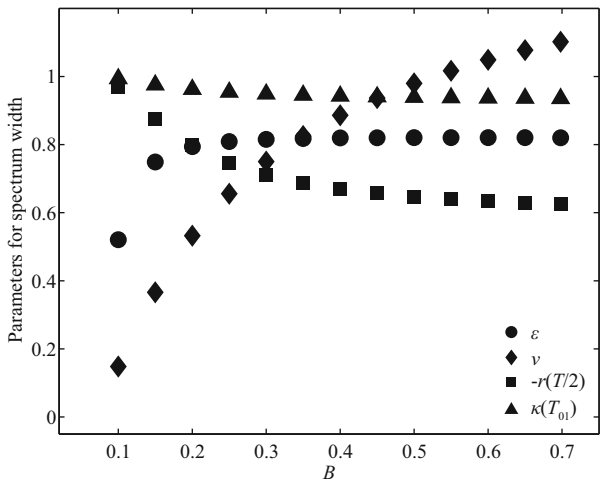

Fig.7 Relationship between different spectrum-width parameters

value is H_{rms}/m =8. Another important relation is the ratio between H_s and $m_0^{1/2}$, which has widespread application in remote sensing, numerical prediction, and some other aspects of wave heights. For narrowband waves, this relation is given as Eq.2. The dependences of these two ratios on B will be investigated in this section.

For the statistical calculation in this section, we employed σ, which is a statistical parameter of the surface time series, rather than m_0, which is calculated from the spectrum, because H_{rms} and H_s are also derived statistically from the surface time series. We first checked the consistency between m_0 and σ^2, and found that the m_0/σ^2 ratios for various B are close to unity with an average value of 1.002 (Fig.5).

The ratios of H_{rms}/σ for various B are shown in Table 1 and Fig.5 in reciprocal forms. This ratio declines at a decreasing rate with B. For fully grown wind waves, it reaches a value of 7.368, which is about 92.1% of that for B=0. A polynomial regression was processed to provide an empirical relation between H_{rms}/σ and B as

$$H_{\mathrm{rms}}^2/\sigma^2 = 8.043 - 2.123B + 1.526B^2 + 0.244B^3 . \quad (13)$$

The ratio of H_s/σ also declines with B (Fig.6). For fully grown wind waves, it reaches a value of 3.825, which is about 95.5% of that for B=0. This means that values of H_s predicted from σ with Eq.2 are 4.7% higher than the real values for fully grown wind waves. The empirical relation between them is given as

$$H_s/\sigma = 4.011 - 0.717B + 0.955B^2 - 0.438B^3 . \quad (14)$$

4 DISCUSSION

There have been several spectrum-width parameters defined by previous researchers. Here, four typical parameters are selected for comparison with B: $\varepsilon = \left(1 - m_2^2/m_0 m_4\right)^{1/2}$ (Cartwright and Longuet-Higgins, 1956), $\nu = \left(m_2/m_0\right)^{1/2}\left(\tau/2\pi\right)$ (Longuet-Higgins, 1975), $r\left(\frac{T}{2}\right) = R\left(\frac{T}{2}\right)/\sigma_0^2$ (Naess, 1985), and $\kappa\left(T_{01}\right) = \left(\begin{array}{l}\left|m_0^{-1}\int_0^\infty S(f)\cos 2\pi f T_{01}\mathrm{d}f\right|^2 \\ +\left|m_0^{-1}\int_0^\infty S(f)\sin 2\pi f T_{01}\mathrm{d}f\right|^2\end{array}\right)^{1/2}$ (Goda and Kudaka, 2007), where S and m_n are the wave spectrum and its n-th moment; σ_0 and R are the standard deviation and autocorrelation function of wave elevation; τ, T, and T_{01} are the mean wave period, dominant wave period, and m_0/m_1, respectively. Values of these parameters for various B, calculated from their definitions, are listed in Table 1. The comparison between these parameters and B is shown

in Fig.7. Among these parameters, v displays the most obvious variation with the increase of B (i.e., with growth of wind waves). This might be because v is defined as the energy concentration degree around a certain frequency, which varies more obviously than the other parameters with the growth of wind waves and the transform of the wind-wave spectrum. Within the wind-wave scope, ε varies in the interval (0, 0.821], v varies in (0, 1.102], $\kappa(T_{01})$ varies in [0.931, 1), and $r(T/2)$ varies in (-1, -0.624].

Some of the abovementioned authors also estimated the H_s/σ ratio based on their theoretical or empirical results (Goda and Kudaka, 2007; Alkhalidi, 2012). Our results are comparable with these in terms of magnitude and trends, which indirectly proves the validity of our results.

One of the advantages in describing spectrum width with B is that the calculation of B only involves the lowest moment of the spectrum and thus, it is much simplified. Another advantage is that as a factor in the spectrum expression, B could be derived empirically from wind parameters in conjunction with other factors (Wang and Hou, 2008). Furthermore, the introduction of B benefits the construction of a wave spectrum for wind waves in different growth stages, just as has been done in this paper.

The fact that B can be derived from wind field states is beneficial to the remote sensing of H_s. In retrieval algorithms for H_s, an important step is the recovery of H_s from the measured σ, which is calculated using Eq.2 (Wang et al., 1995). As shown in the last section, using Eq.2 could induce overestimations in H_s of up to 4.7%. This error would be significant under the condition of strong winds and severe sea states. An accurate estimation of B from surface wind fields acquired remotely, in conjunction with the use of Eq.14, could efficiently improve the accuracy of an H_s retrieval algorithm, especially for situations of severe sea states.

The methods used in this paper still assume linear waves. The effect of nonlinearity on the probability distribution of wind-wave heights with different B needs further investigation. Furthermore, the shallow water effect and bimodal spectrum form, corresponding to mixed sea states, are also not discussed in this paper.

5 CONCLUSION

A wave-spectrum-width parameter B was introduced into the JONSWAP spectrum to facilitate the construction of wind-wave spectra for various growth stages, i.e., between B=0 for newly created wind waves and B=0.698 1 for fully grown wind waves.

The time series of sea surface displacements were then reconstructed from the spectra and the probability density distributions of the wind-wave heights were studied statistically. The distribution curves deviated slightly from the theoretical Rayleigh distribution with increasing B. The probability that wave heights exceed a certain value was clearly smaller than the theoretical value for $B\geq$0.3, and the difference between them increased with the threshold value.

The relation between the H_s/σ ratio and B was investigated based on the statistics. The H_s/σ ratio deviated from 4.005 and declined with B. When the value of B reached 0.698 1, the H_s/σ ratio reached 3.825, which is about 95.5% of its original value. This indicates an overestimation in the prediction of H_s by Eq.2 from σ, and provides a potential method for improving the accuracy of the H_s remote sensing retrieval algorithm, critical for extremely large waves under severe sea states.

References

Alkhalidi M A, Tayfun M A. 2013. Generalized Boccotti distribution for nonlinear wave heights. *Ocean Engineering*, **74**: 101-106.

Alkhalidi M A. 2012. Asymptotic wave-height distributions and conditional statistics. *Kuwait University Journal of Science and Engineering*, **39**: 79-92.

Boccotti P. 2012. A new property of distributions of the heights of wind-generated waves. *Ocean Engineering*, **54**: 110-118.

Cartwright D E, Longuet-Higgins M S. 1956. The statistical distribution of the maxima of a random function. Proceedings of the Royal Society of London. Series A. Mathematical and Physical Sciences, **237**(1209): 212-232.

Chakrabarti S K, Cooley R P. 1977. Statistical distribution of periods and heights of ocean waves. *Journal of Geophysical Research*, **82**(9): 1 363-1 368.

Earle M D. 1975. Extreme wave conditions during Hurricane Camille. *Journal of Geophysical Research*, **80**(3): 377-379.

Forristall G Z. 1978. On the statistical distribution of wave heights in a storm. *Journal of Geophysical Research*, **83**(C5): 2 353-2 358.

Goda Y, Kudaka M. 2007. On the role of spectral width and shape parameters in control of individual wave height distribution. *Coastal Engineering Journal*, **49**(3): 311-335.

Goda Y. 1970. Numerical experiments on wave statistics with spectral simulation. *Report of the Port and Harbour Research Institute*, **9**(3): 3-57.

Haring R E, Osborne A R, Spencer L P. 1976. Extreme wave parameters based on continental shelf storm wave records. Proceedings of 15th Conference on Coastal Engineering, Honolulu, Hawaii.

Hasselmann K, Barnett T P, Bouws E, Carlson H, Cartwright D E, Enke K, Ewing J A, Gienapp H, Hasselmann D E, Kruseman P, Meerburg A, Müller P, Olbers D J, Richter K, Sell W, Walden H. 1973. Measurements of wind-wave growth and swell decay during the Joint North Sea Wave Project (JONSWAP). Ergänzungsheft 8-12. Hamburg, Deutsches Hydrographisches Institut. 95p.

Hou Y, Guo P, Song G, Song J, Yin B, Zhao X. 2006. Statistical distribution of nonlinear random wave height. *Science in China Series D*, **49**(4): 443-448.

Hou Y, Wen S. 1990. Wind wave spectra with three parameters. *Oceanologia et Limnologia Sinica*, **21**(6): 495-504. (in Chinese with English abstract)

Huang N E, Long S R, Tung C-C, Yuan Y, Bliven L F. 1983. A non-Gaussian statistical model for surface elevation of nonlinear random wave fields. *Journal of Geophysical Research*: *Oceans*, **88**(C12): 7 597-7 606.

Izadparast A H, Niedzwecki J M. 2013. Four-parameter Weibull probability distribution model for weakly non-linear random variables. *Probabilistic Engineering Mechanics*, **32**: 31-38.

Larsen L H. 1981. The influence of bandwidth on the distribution of heights of sea waves. *Journal of Geophysical Research*: *Oceans*, **86**(C5): 4 299-4 301.

Longuet-Higgins M S. 1952. On the statistical distributon of the height of sea waves. *Journal of Marine Research*, **11**(3): 245-266.

Longuet-Higgins M S. 1963. The effect of non-linearities on statistical distributions in the theory of sea waves. *Journal of Fluid Mechanics*, **17**(3): 459-480.

Longuet-Higgins M S. 1975. On the joint distribution of the periods and amplitudes of sea waves. *Journal of Geophysical Research*, **80**(18): 2 688-2 694.

Longuet-Higgins M S. 1980. On the distribution of the heights of sea waves: some effects of nonlinearity and finite band width. *Journal of Geophysical Research*, **85**(C3): 1 519-1 523.

Naess A. 1985. On the distribution of crest to trough wave heights. *Ocean Engineering*, **12**(3): 221-234.

Pierson Jr. W J, Moskowitz L. 1964. A proposed spectral form for fully developed wind seas based on the similarity theory of SA Kitaigorodskii. *Journal of Geophysical Research*, **69**(24): 5 181-5 190.

Tayfun M A, Fedele F. 2007. Wave-height distributions and nonlinear effects. *Ocean Engineering*, **34**: 1 631-1 649.

Tayfun M A. 1980. Narrow-band nonlinear sea waves. *Journal of Geophysical Research*: *Oceans*, **85**(C3): 1 548-1 552.

Tayfun M A. 1990. Distribution of large wave heights. *Journal of Waterway*, *Port*, *Coastal*, *and Ocean Engineering*, **116**(6): 686-707.

Wang G, Wang H, Xu G. 1995. The Principle of the Satellite Altimetry. Science Press, Beijing. 390p. (in Chinese)

Wang X, Hou Y. 2008. The developing model of wind wave spectrum: Part I. The growth relation between spectrum parameters and fetch. *Oceanologia et Limnologia Sinica*, **39**(5): 433-438. (in Chinese with English abstract)